Centrosome fragments and microtubules are transported asymmetrically away from division plane in anaphase

Nasser M. Rusan and Patricia Wadsworth

Department of Biology and Program in Molecular and Cellular Biology, University of Massachusetts, Amherst, MA 01003

Spinning disc confocal microscopy of LLCPK1 cells expressing GFP-tubulin was used to demonstrate that microtubules (MTs) rapidly elongate to the cell cortex after anaphase onset. Concurrently, individual MTs are released from the centrosome and the centrosome fragments into clusters of MTs. Using cells expressing photoactivatable GFP-tubulin to mark centrosomal MT minus ends, a sevenfold increase in MT release in anaphase is documented as compared with metaphase. Transport of both individually released MTs and clusters of MTs is directionally biased: motion is directed away from the equatorial region. Clusters of MTs retain centrosomal components at their focus and the capacity to nucleate MTs. Injection of mRNA encoding nondegradable cyclin B blocked centrosome fragmentation and the stimulation of MT release in anaphase despite allowing anaphase-like chromosome segregation. Biased MT release may provide a mechanism for MT-dependent positioning of components necessary for specifying the site of contractile ring formation.

Introduction

During each somatic cell cycle, the long, stable microtubules (MTs) of the interphase array are replaced with a mitotic spindle composed of short, dynamic MTs. Much attention has been focused on MT behavior and chromosome motion during spindle assembly (Compton, 2000; Karsenti and Vernos, 2001; Rieder and Khodjakov, 2003). In contrast, MT behavior during mitotic exit has been less well characterized, despite the importance of these changes for successful completion of the cell cycle.

During mitotic exit, kinetochore MTs shorten, the number of centrosome-associated MTs decreases to interphase levels (O'Toole et al., 2003), and astral MTs increase in length (Canman et al., 2003). Despite these dramatic changes in MT organization, polymer level remains constant as cells progress from mitosis to G1 (Zhai et al., 1996). This suggests that assembly and disassembly are balanced in the cell as a whole, that existing MTs are reorganized to form interphase arrays, or a combination of both processes (Rusan et al., 2002; Tulu et al., 2003).

To determine how the MT array is remodeled at the exit from mitosis, we examined MT behavior in cells progressing from anaphase through telophase using both live-cell analysis and three-dimensional (3D) reconstruction of fixed material. Our results demonstrate that during the transition from metaphase to interphase, released MTs and pole fragments are transported asymmetrically away from the site of contractile ring formation.

The online version of this article includes supplemental material.

Correspondence to Patricia Wadsworth: patw@bio.umass.edu

Abbreviations used in this paper: 3D, three dimensional; MT, microtubule.

Results and discussion

To examine spindle disassembly as cells progress from metaphase to interphase, we imaged LLCPK1 epithelial cells expressing GFP-α-tubulin (LLCPK1-α; Rusan et al., 2001). Metaphase cells were located and followed by phase-contrast microscopy for timing of anaphase onset (Fig. 1, top panels), then spinning disk confocal microscopy was used to follow GFP-tagged tubulin (Fig. 1, middle panels). We observed three distinct behaviors after anaphase onset. First, immediately after anaphase onset, MTs elongate toward the cell cortex before resuming dynamic instability (Fig. 1 A; Fig. S1 and Video 1, available at http://www.jcb.org/cgi/content/full/jcb.200409153/DC1; see also Canman et al., 2003). Second, as the cell progresses through anaphase and into telophase, the centrosome becomes less compact, as clusters of MTs detach and move away from the centrosome (Fig. 1 B). Third, extensive release of individual MTs and their movement away from the centrosome was detected immediately after anaphase onset (Fig. 1 C). Release of individual MTs and fragmentation of the spindle pole are mechanisms that contribute to remodeling the MT array at exit from mitosis.

The Journal of Cell Biology, Vol. 168, No. 1, January 3, 2005 21–28
http://www.jcb.org/cgi/doi/10.1083/jcb.200409153

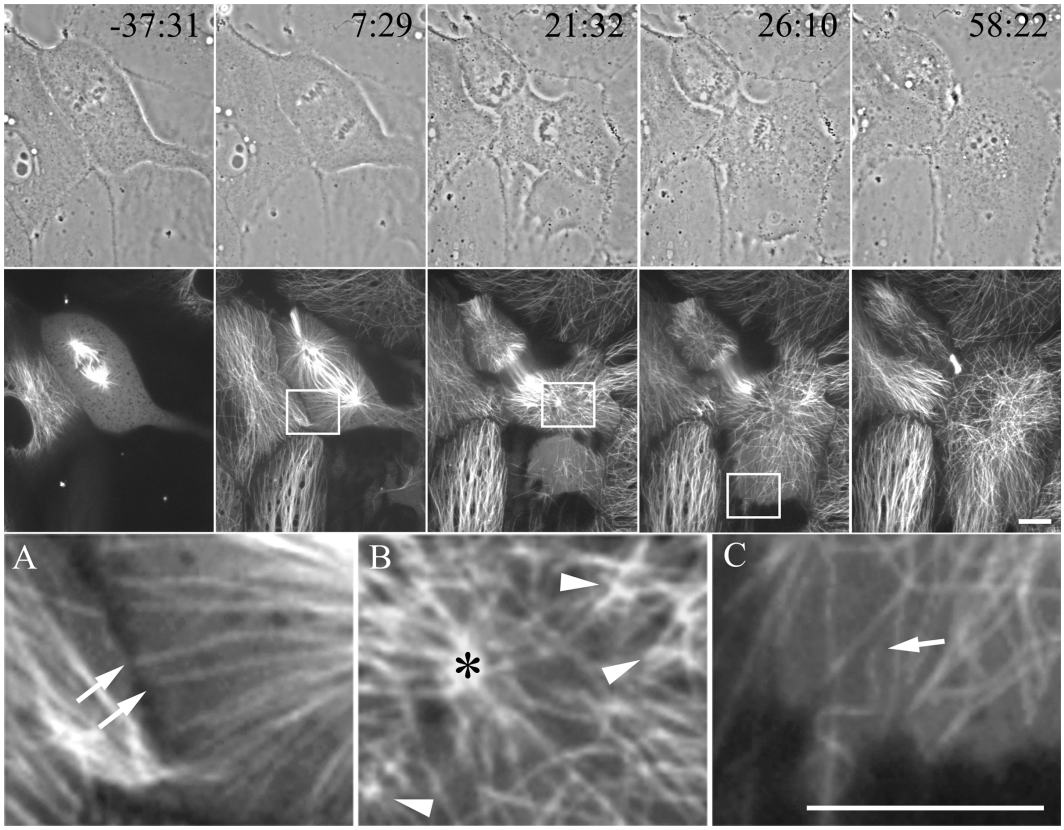

Figure 1. **Remodeling the MT array in anaphase.** Phase-contrast (top) and corresponding fluorescence images (middle) of an LLCPK1-α cell during exit from mitosis. (A–C) Enlargements of the boxed regions in the images above. (A) After anaphase onset, astral MTs elongate toward the cortex (arrows) and (B) clusters of MTs (arrowheads) detach and move away from the centrosome (asterisk). (C) Optical sections just above the cell membrane revealed a large number of short MTs with two free ends (arrow). Time (in min:sec) is relative to anaphase onset. Bar, 10 μm.

MT release from the centrosome in anaphase cells

To investigate MT release from the centrosome in anaphase, we examined MT distribution in fixed cells and MT behavior in LLCPK1-α cells. Confocal images of the entire cell volume of anaphase cells fixed and stained with antibodies against tubulin revealed a large number of short noncentrosome-associated MTs in Z-sections along the lower cell cortex (Fig. 2 A); this population of MTs was not detected in metaphase cells (unpublished data). Time-lapse sequences of living LLCPK1-α cells show extensive MT release from the centrosome, accounting for the presence of short, noncentrosome-associated MTs in fixed cells (Fig. 2 B, Video 2). In live cells, the dissociation of minus ends of existing MTs, and newly nucleated MTs, from the centrosome is clearly observed (Fig. 2 B, colorized MTs). Because a MT could be followed throughout the process of nucleation and release, it was evident that the movement was plus-end leading.

Release events are of two types (Rodionov and Borisy, 1997): in some cases, plus-end growth and apparent attachment to the cortex is followed by minus-end release and disassembly (Fig. 2 B, pink MT, arrow). Other MTs are released before the plus end reaches the cortex (Fig. 2 B, yellow MT) and move swiftly along the cortex, exhibiting straight, twisting, circular, and sometimes flagella-like movements. In some cases, the freely moving plus ends encounter the cortex and become stabilized while the minus end undergoes apparent disassembly, similar to the first type (Fig. 2 B, red and green MTs). The majority of released MTs are completely disassembled, whereas the rest are either stabilized or were not followed long enough to determine their fate.

Previous work has shown that MT release from the centrosome is infrequent in interphase and mitotic cells: ~1/min and 0.05/min, respectively (Keating et al., 1997; Rusan et al., 2001). Our observations demonstrate a marked increase in MT release in anaphase, a phenomenon that may function to reduce the number of centrosomal MTs and to reestablish the interphase array. At all stages of the cell cycle, however, MT release is difficult to quantify given the density of MTs in the centrosomal region.

Analysis of MT release using photoactivatable GFP-tubulin

To quantify MT release events and to determine the mechanism by which released MTs are moved, we generated an LLCPK1 cell line that stably expresses photoactivatable GFP-tagged α-tubulin: LLCPK1-PAα (see Materials and methods; Patterson and Lippincott-Schwartz, 2002). Using these cells, we can generate a fiduciary mark on the MT lattice, quantify release events, and determine the mechanism of MT motion.

LLCPK1-PAα cells were photoactivated with violet light restricted by a pinhole placed in the light path; this created a

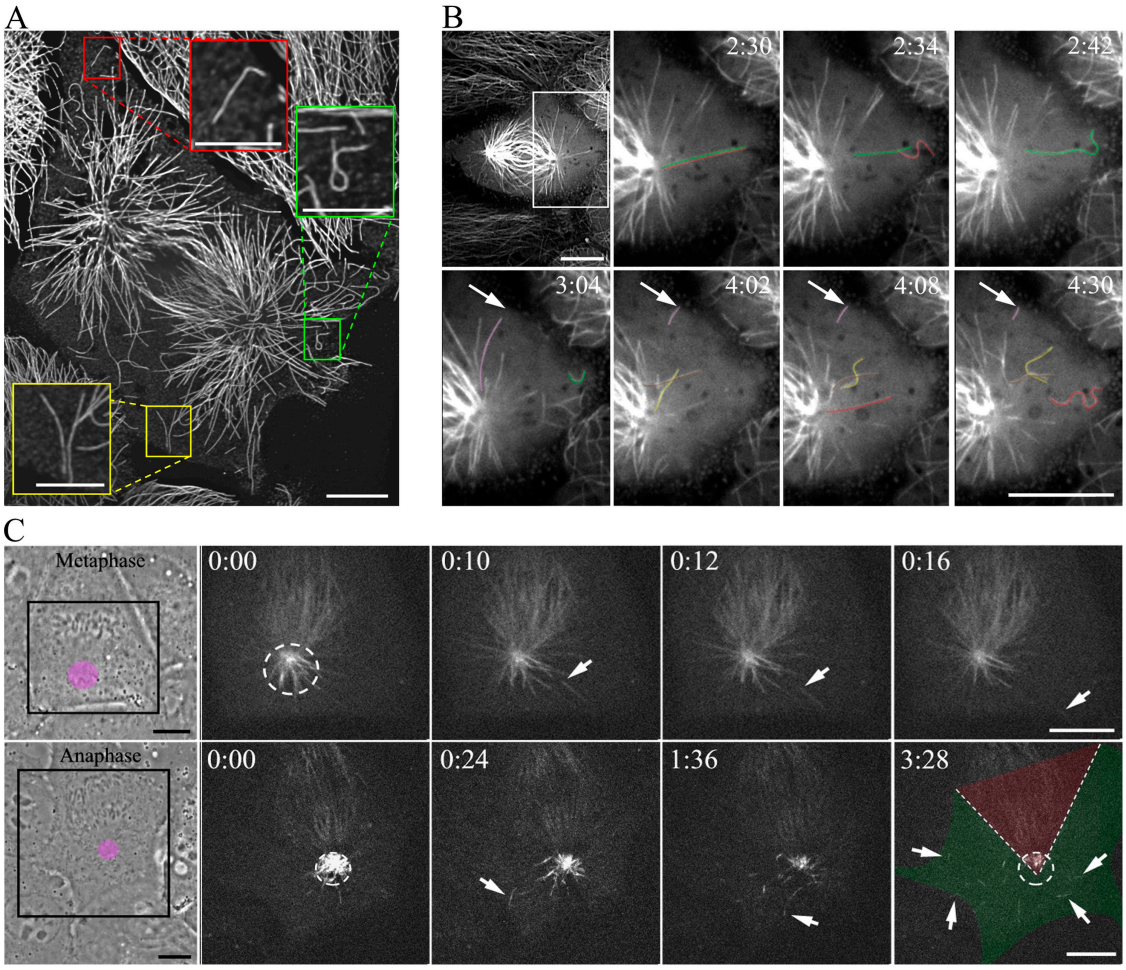

Figure 2. **MT release from the centrosome in anaphase.** (A) Deconvolved image of fixed anaphase cell stained with antibodies to tubulin. Boxed regions, enlarged within the image, show MTs with two free ends. (B) MT release from the centrosome in a living LLCPK1-α cell in anaphase. Some MTs are colored to assist in visualization. Time (in min:sec) is relative to anaphase onset. Bars: 10 μm (all); 5 μm (A, boxed regions). (C) Selected images from time-lapse sequences of a metaphase and an anaphase cell expressing PA-GFP tubulin; area of photoactivation shown in violet. Released MTs are indicated with white arrows. At time 3:28, the polar (green) and chromosomal (red) regions are indicated. The activation shown in C is the second activation of each cell, explaining the fluorescence in the spindle at time zero. Bars, 10 μm.

5-μm-diameter activation mark that was centered around the centrosome (Fig. 2 C, violet circle). In metaphase cells, we observed a rapid dissipation of fluorescence in the activated region, consistent with the rapid dynamics of metaphase MTs (Saxton et al., 1984). Occasionally, a fluorescent mark was seen to exit the activated region and travel through the cytoplasm (Fig. 2 C, metaphase; see Video 3). The rate of MT release (2.9/min; Table I) was calculated by counting the number of release events in the first 10-s post-photoactivation. Within the first 10 s, the measured number of releases/min is the most accurate because it limits the number of newly nucleated (and thus nonfluorescent) MTs that might be undetectably released.

In anaphase cells, we observed a dramatic loss of fluorescence as MTs were transported out of the photoactivated region (Fig. 2 C; see Video 4). The behavior of photoactivated MTs was indistinguishable from released MTs in anaphase LLCPK1-α cells (Fig. 2 B), exhibiting twisting and turning movements. From these movies we measured a rate of release (19.2 releases/min) that was approximately sevenfold greater than in metaphase (Table I). It was difficult to accurately determine the rate of motion of the released MTs because of their erratic behavior; however, we estimate the rate to be 20–60 μm/min. These data demonstrate that the rate of MT release is regulated throughout the cell cycle and that previous measurements of MT release in cells containing uniformly fluorescent MTs greatly underestimate the frequency of MT release, at least in mitotic cells (Rusan et al., 2001).

Released MTs are transported

PA marks were observed to move from the centrosomal region to the polar region of the cell, implicating transport as the mechanism for moving released MTs. If treadmilling alone were responsible for movement, the 2–3-μm PA mark on the MTs' minus end would be lost as a result of minus-end disassembly. Some marks are retained until the end of the movie, whereas others are completely disassembled, indicating that MT minus ends can switch to disassembly after (or during) release and transport. Released and stabilized MTs may serve as precursors to the noncentrosomal interphase array (Bacallao et al., 1989; Ahmad and Baas, 1995). Also, some PA fluorescence

Table I. **Measurements of MT release and cluster motion in anaphase**

	Frequency of release		Rate of MT motion
	Metaphase	Anaphase	
	releases/min	*releases/min*	*μm/min*
GFP-tubulin	0.05[a]	5.51 (n = 11 poles)	-
PA-GFP-tubulin	2.9 (n = 6 poles)	19.2 (n = 5 poles)	-
Released MTs	-	-	∼ 20–60
MT clusters	-	-	2.6 ± 1.2 (n = 18 clusters, 12 cells)

[a]Rusan et al., 2001.

was retained at the centrosome and dissipated over time without apparent movement; this could result from minus-end disassembly of MTs that were released and not transported, or from catastrophic disassembly of MT plus ends.

The behavior of released MTs is consistent with transport by a cortically tethered minus-end motor (Keating et al., 1997; Grill et al., 2003). Cytoplasmic dynein has been implicated in MT transport in neurons, egg extracts, and cultured cells and in positioning the spindle in various cell types (Ahmad et al., 1998; Bloom, 2001; Abal et al., 2002; Gonczy, 2002), and may contribute to MT transport in anaphase cells as well.

Asymmetric transport away from the division plane

Observations of MT release in LLCPK1-α and LLCPK1-PAα suggested that MT release from the centrosome was asymmetric. To quantify the directionality of release events, anaphase cells were photoactivated and the number of release events were counted in two regions: the chromosomal region, which extended from the centrosome toward the lateral cortex at the cell equator (encompassing the chromosomes), and the polar region (Fig. 2 C, red and green regions, respectively). In no case (n = 5 cells, 135 release events) was a released MT transported into the chromosomal region; this includes both MTs that might be directly released into the chromosomal region or ones that were released elsewhere and subsequently moved into the chromosomal region. Subdividing the polar region into five regions of ∼60° (unpublished data) showed that release was uniform throughout the polar region. Further, examination of the activated zone shows that fluorescence dissipation in the chromosomal area is slower than the polar region (Fig. 2 C, compare red and green zones). These results demonstrate that anaphase MTs are released and transported with directional bias away from the chromosomal region.

The high release rate in the polar region increases MT turnover by creating new free minus ends. In contrast, in the equatorial/chromosomal region, where release is not observed, MTs would be comparatively more stable. This observation is consistent with recent work demonstrating that MTs extending toward the furrow are more stable than MTs elsewhere in the late anaphase cell (Canman et al., 2003). We suggest that the bias in MT release and turnover can differentially affect cortical contractility, and thus may contribute to specification of the site of contractile ring formation (Glotzer, 2004).

Centrosome fragmentation in anaphase cells

Our initial observations of anaphase cells demonstrated that in addition to release of individual MTs, the centrosome fragments into MT clusters. These clusters were transported radially away from the centrosomes to the cell periphery, populating areas devoid of MTs in metaphase (Fig. 3 A; Videos 5 and 6). Transport was stochastic, with periods of faster movement interrupted by slower movements and pauses (Fig. 3 C; Table I). Similar to individual MT release, in no case was a cluster observed to move into the chromosomal region (Fig. 3 B). Analysis of MT clusters in LLCPK1-α anaphase cells showed that the extending MT-ends undergo dynamic instability, indicating that these MTs are oriented with the plus ends facing outward. Occasionally a cluster disassembles, releasing individual MTs, which then behaved identically to those released from the centrosome.

To determine the 3D organization of centrosome fragments, cells were fixed and stained with an antibody against tubulin and the entire cell volume was imaged using spinning disk confocal microscopy and subjected to blind-iterative deconvolution. Maximum intensity projections and 3D reconstructions of these cells revealed clusters of MTs (Fig. 3 D), composed of three to several tens of MTs that meet at a common focus, consistent with our observations in live cells.

Our observation of centrosome fragmentation at mitotic exit in mammalian cells is consistent with recent findings of centrosome disassembly in *Xenopus* and yeast (Cao et al., 2003; Cheeseman and Desai, 2004; Zimmerman et al., 2004), indicating that this may be a conserved feature of mitosis in diverse cells. Cell cycle–dependent inactivation or destruction of centrosomal components may regulate centrosome disassembly in mammalian cells, as observed in other cell types.

Centrosomal proteins at the foci of MT clusters

Because the MT clusters originated from the centrosome, we tested the possibility that centrosome and spindle pole components were present at their foci. From live imaging of an LLCPK1 cell line stably expressing GFP-γ-tubulin (Fig. S2 A)

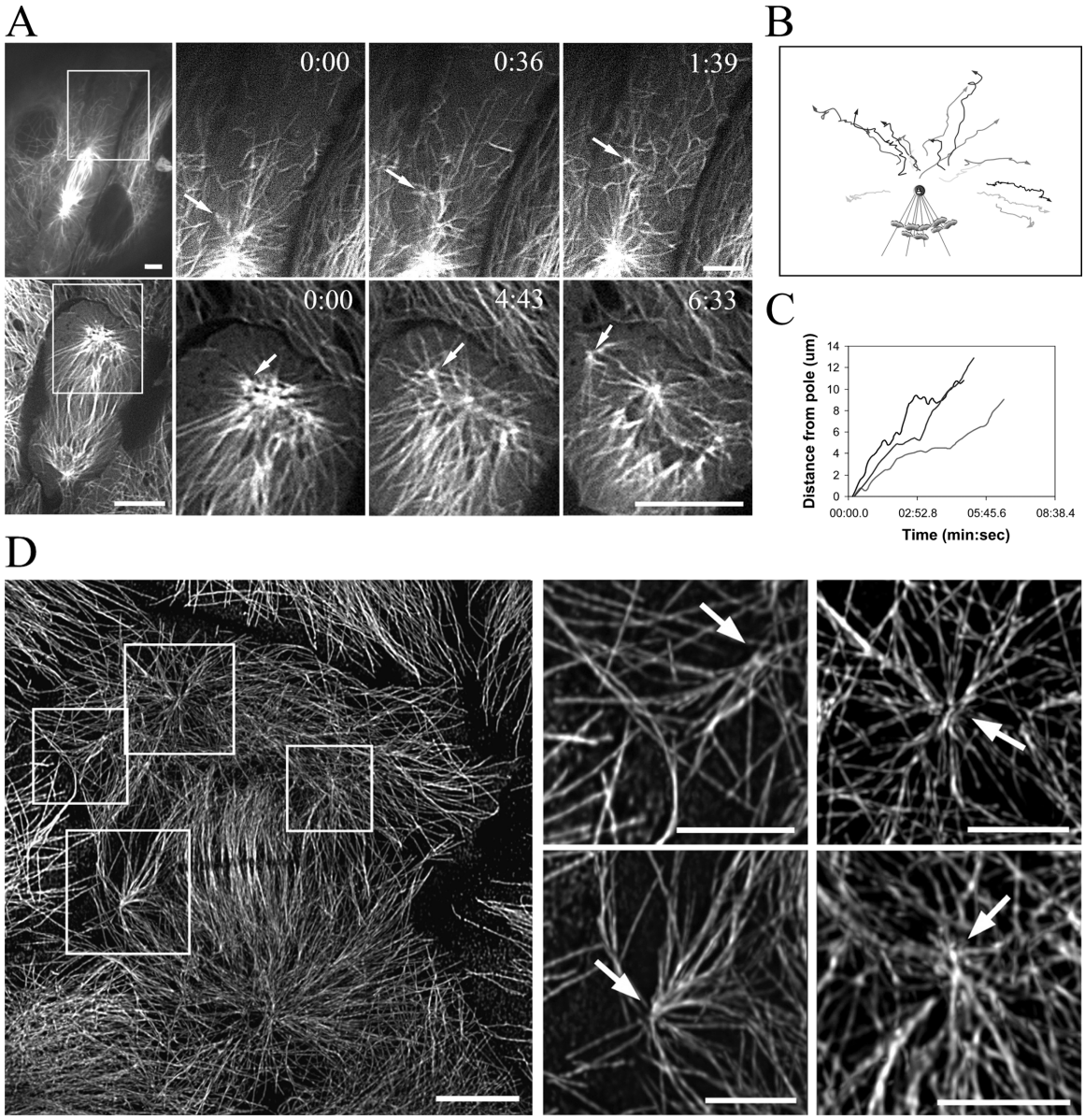

Figure 3. **Centrosome fragmentation in anaphase cells.** (A) Selected images from time-lapse sequences of living LLCPK1-α cells showing centrosome fragmentation (arrows); time (in min:sec) is relative to anaphase onset. (B) x,y coordinates were used to generate traces of the paths of all clusters from 12 cells. (C) Life history plots (distance vs. time) for three representative clusters. (D) Deconvolved image showing MT clusters (boxed regions), each with a common focus (arrows). Bars: 10 μm (all); 5 μm (A, right panels).

we did not observe GFP-γ-tubulin fluorescence moving away from the centrosome, presumably because the weak GFP signal was not detectable. However, using immunofluorescence, γ-tubulin was detected at the foci of noncentrosomal MT clusters and at the centrosome (Fig. S2 C). This indicates that γ-tubulin is retained by the foci and transported away from the centrosome, effectively decreasing its levels there (Khodjakov and Rieder, 1999; Grill et al., 2003; Zimmerman et al., 2004).

The centrosomal proteins pericentrin and ninein localize to the foci of MT clusters as well as the centrosomes in anaphase (Fig. S2 C; Mogensen et al., 2000). Immunolocalization of NuMA (Merdes et al., 1996) revealed its accumulation at spindle poles in metaphase and its dispersion in anaphase and telophase (Fig. S2 C), which temporally corresponds to centrosome fragmentation and cluster movement. NuMA is not restricted to the foci of MT clusters, but is localized to MTs near the fragmented poles.

Centrosome fragments nucleate MTs

The presence of centrosomal components in the MT clusters suggests that they retain the capacity to nucleate MTs. To examine this possibility we used an LLCPK1 cell line permanently expressing the plus end–binding protein EB1 tagged to GFP (Piehl and Cassimeris, 2003). Previous live imaging of this line revealed the presence of extra nucleation sites in mitotic cells (Piehl et al., 2004). In anaphase cells, extra nucleation sites were observed originating from the centrosome and moving outward (Fig. 4 B; Videos 7 and 8) into the polar region

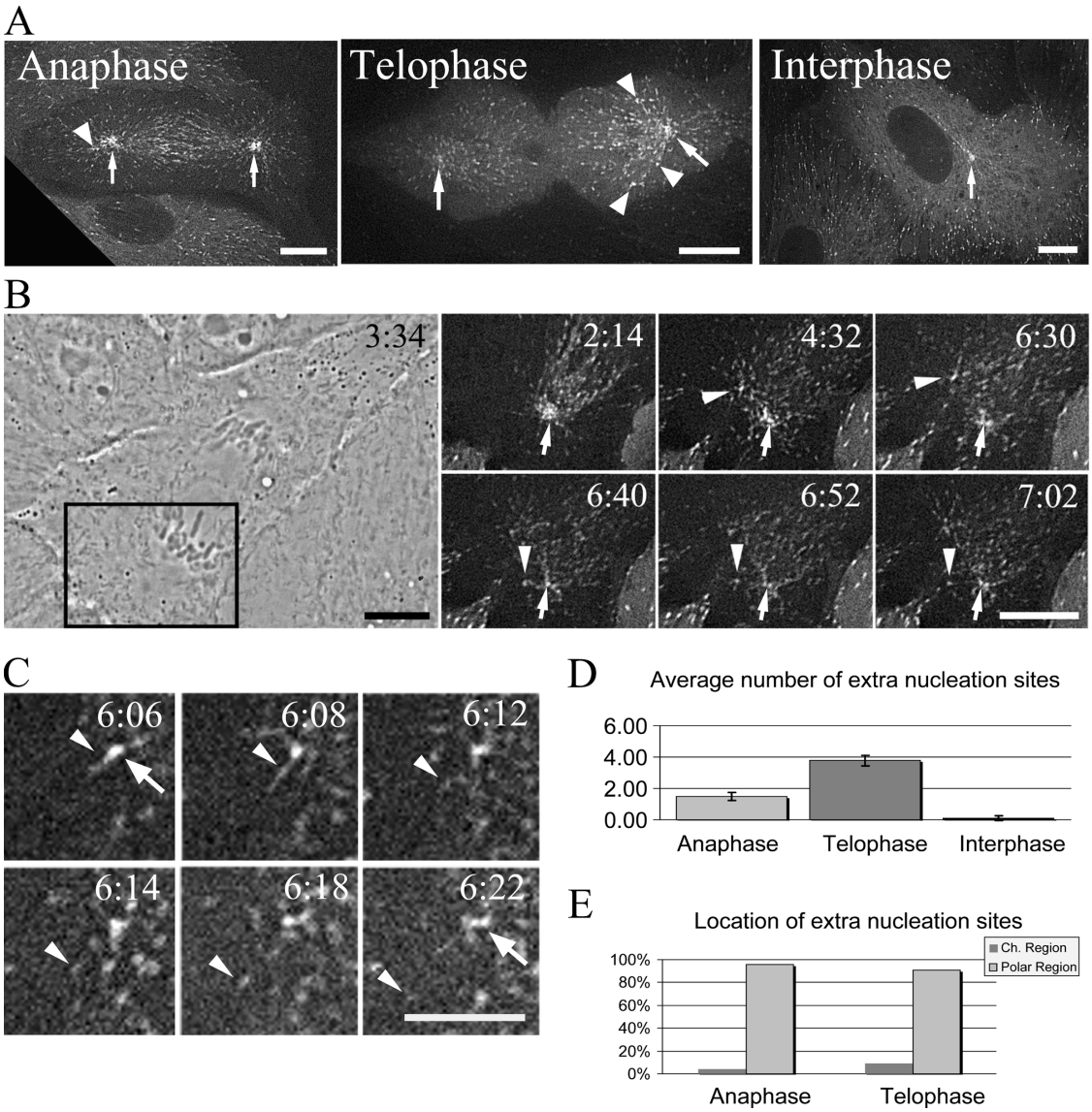

Figure 4. **MT clusters nucleate MTs.** (A) Fluorescence images of LLCPK1-EB1-GFP cells; arrows show centrosomes, arrowheads show extra nucleation sites. (B) Movement of extra nucleation sites away from the centrosome, boxed region in phase image is shown on right; examples of two sites. Arrowheads show extra sites and arrows indicate centrosomes. (C) Individual nucleation events at an extra nucleation site. Arrow indicates the extra nucleation site and the arrowhead marks an EB1-GFP dash. (D) Quantification of the number of extra nucleation sites. (E) Location of extra nucleation sites was classified as chromosomal or polar. Bars: 10 μm (A and B); 5 μm (C).

(Fig. 4 E). Centrosome fragments continued to nucleate MTs as they moved away from the centrosome (Fig. 4 C). Quantification of extra nucleation sites from image sequences of anaphase, telophase, and interphase cells revealed averages of 1.5, 4.0, and 0.21 sites/cell, respectively (Fig. 4, A and D). The increased number of nucleation sites in telophase, as compared with anaphase, shows that pole fragmentation is maximal in telophase cells (Fig. 4 D). The observation that extra nucleation sites were extremely rare in interphase cells (Fig. 4 D) suggests that all extra nucleation sites are ultimately disassembled.

Pole fragmentation and MT release are regulated by Cdk1 activity

Previous studies have shown that inactivation of CDK1 is required for the conversion of a mitotic array to an interphase array and for cytokinesis (Verde et al., 1990; Murray et al., 1996; Wheatley et al., 1997), suggesting that CDK1 inactivation may be required for MT release and pole fragmentation. To test this possibility, early prometaphase LLCPK1-α cells were injected with mRNA encoding a nondegradable form of cyclin B (cyclin BΔ90), imaged, and analyzed for release events and centrosome fragmentation. In all cases (9/9), sister chromatids in the injected cell separated normally (Murray et al., 1996; Wheatley et al., 1997), but the centrosome and spindle poles remained intact for the duration of the time-lapse movies, with no significant fragmentation occurring (Fig. 5 A; Video 9). Occasionally, the pole would split into two or three mini-poles, and some MT bundles would form in the surrounding cytoplasm. However, these events were insufficient for repopulating the cytoplasm with MTs and the cell maintained a metaphase-like morphology.

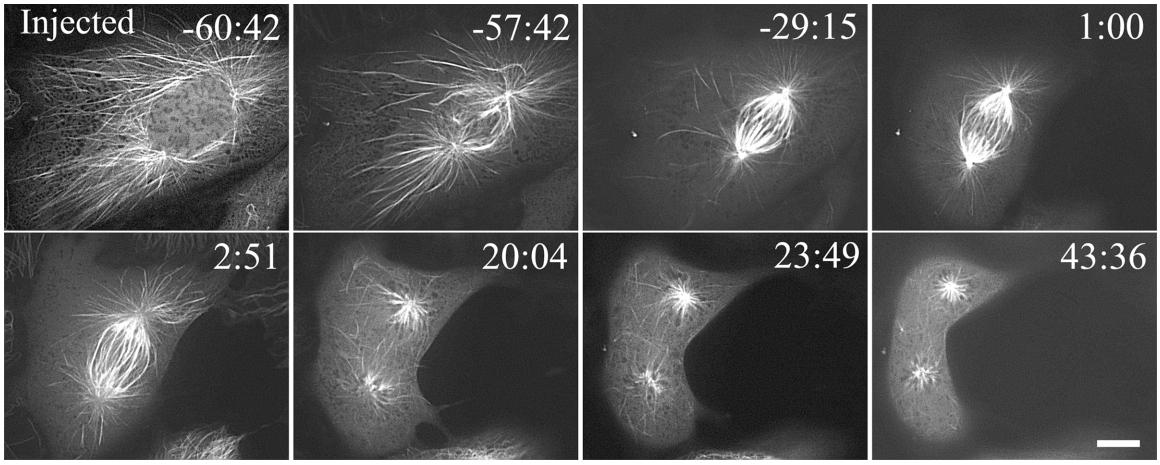

Figure 5. **Inactivation of CDK1 is required for MT release and centrosome fragmentation in anaphase.** Selected frames from a time-lapse sequence of an LLCPK1-α cell injected at prophase with mRNA encoding cyclin BΔ90; centrosome fragmentation and MT release are inhibited and two independent half-spindles remain in the cell. Time is relative to anaphase onset. Bar, 10 μm.

MT release events, which occur along the lower cell cortex, were difficult to image because cyclin BΔ90–injected cells remained rounded. However, in cells with a flat morphology ($n = 2$) the number of release events was significantly reduced (Video 10) when compared with control anaphase cells. Consistent with previous work, injected cells showed abnormal and/or delayed cytokinesis, persistent condensed chromosomes, and oscillation of single sister chromatids (Murray et al., 1996; Wheatley et al., 1997). Control injections of luciferase mRNA had no detectable effect on mitotic exit ($n = 4$ cells). Interestingly, injection of cyclin BΔ90 at metaphase did not prevent the repopulation of the cell periphery with MTs, presumably because the level of translated cyclin BΔ90 was insufficient to activate CDK1. However, with time the peripheral MTs were moved inward, and a metaphase-like MT array was reestablished (Fig. S3).

Summary

MT release and centrosome fragmentation at mitotic exit provide a mechanism to reduce the number of centrosomal MTs and to contribute to the reestablishing of the interphase array. The directional bias in MT release and transport generates local differences in MT stability, which could contribute to determining the site of contractile ring formation.

Materials and methods

Materials

Materials for cell culture were obtained from Invitrogen, with the exceptions of Ham's F10 and antibiotics, which were obtained from Sigma-Aldrich, and FBS, which was obtained from Atlanta Biologicals. All chemicals were obtained from Sigma-Aldrich.

Cell culture

LLCPK1-α cells were cultured in a 1:1 mixture of Opti-MEM/Ham's F10 media supplemented with 7.5% FBS and antibiotics. Cells were grown in a 5% CO_2 atmosphere at 37°C. Cells were plated on coverslips 2 d before imaging, mounted in chambers, and placed on a heated stage. A permanent cell line expressing PA-GFP-tubulin was generated as described previously (Goodson and Wadsworth, 2004), using a PA-GFP construct provided by Dr. J. Lippincott-Schwartz (National Institutes of Health, Bethesda, MD).

In vitro transcription

A pET3b vector containing truncated cyclin B (pT7Δ90) was obtained from Dr. Yu-Li Wang (University of Massachusetts Medical School, Worcester, MA). The mMESSAGE mMACHINE kit was used to transcribe the linearized cyclin BΔ90 template (Ambion, Inc.). mRNA product was run through the RNeasy RNA cleanup kit (QIAGEN) to remove unincorporated nucleotides. RNA was eluted using RNase-free water and the concentration was determined by spectrophotometry. The final product was stored at −80°C.

Image acquisition

Images were acquired with a microscope (Eclipse TE300; Nikon) equipped with a 100× phase, 1.4 NA objective lens, a spinning disk confocal scan head (PerkinElmer), and a MicroMax Interline Transfer cooled CCD camera (Roper Scientific). Imaging of live cells was performed as described previously (Rusan et al., 2002).

For photoactivation experiments, cells expressing PA-GFP–tagged tubulin were photoactivated by a 5–7-s exposure to 413-nm light (filter D405/20; Chroma Tech Corp.) from a shuttered 100-W mercury epi-illuminator. The area of photoactivation was restricted using pinholes (Lenox Laser) mounted in a Ludl filter wheel (Ludl Electronic Products) placed in a conjugate image plane.

For 3D reconstruction experiments, fixed cells were imaged with a 100×, NA 1.4 phase objective lens mounted on a p-721 piezo nanofocusing device (Physik Instruments). The entire volume between 1 μm above and 1 μm below the cell was imaged in 200-nm steps and subjected to blind, iterative deconvolution (Autoquant Imaging).

Online supplemental material

Fig. S1 shows MT elongation during anaphase. Fig. S2 shows that MT clusters contain centrosomal proteins at their foci. Fig. S3 shows inactivation of CDK1 in metaphase. The supplemental materials and methods are relevant to supplemental figures. Video 1 shows MT elongation after anaphase onset in LLCPK-1α cells. Corresponds to images presented in Fig. S1. Images were collected every 2 s and displayed at 7.5 frames/s. Video 2 shows MT release from the centrosome in anaphase LLCPK-1α cells. Corresponds to images presented in Fig. 2. Images were collected every 2 s and displayed at 10 frames/s. Video 3 shows MT release from the centrosome in metaphase cells shown by photoactivation of LLCPK-PAα cells. Corresponds to images presented in Fig. 2. Images were collected every 2 s and displayed at 7.5 frames/s. Video 4 shows MT release from the centrosome in anaphase cells shown by photoactivation of LLCPK-PAα cells. Corresponds to images presented in Fig. 2. Images were collected every 3 s and displayed at 10 frames/s. Video 5 shows spindle pole fragmentation and cluster motion in anaphase LLCPK1-α cells. Corresponds to images presented in Fig. 3. Images were collected every 15 s and displayed at 7.5 frames/s. Video 6 shows spindle pole fragmentation and cluster motion in anaphase LLCPK1-α cells. Corresponds to images presented in Fig. 3. Images were collected every 15 s and displayed at 7.5 frames/s. Video 7 shows MT nucleation from centrosome fragments.

Images were collected every 4 s and displayed at 7.5 frames/s. Corresponds to images presented in Fig. 4. Video 8 shows MT nucleation from centrosome fragments (zoomed). Images were collected every 4 s and displayed at 7.5 frames/s. Corresponds to stills in Fig. 4. Video 9 shows that centrosome fragmentation in anaphase requires CDK1 inactivation. Images were collected every 30 s and displayed at 7.5 frames/s. Corresponds to images presented in Fig. 5. Video 10 shows that MT release in anaphase requires CDK1 inactivation. Images were collected every 3 s and displayed at 9 frames/s. Corresponds to images presented in Fig. 5. Online supplemental material available at http://www.jcb.org/cgi/content/full/jcb.200409153/DC1.

We thank Robert Daniels for assistance with in vitro transcription, M. Federico for quantification of extra nucleation sites, C. Fagerstrom for help with immunofluorescence, and U.S. Tulu and Dr. T. Baskin for critically reading this manuscript.

Submitted: 24 September 2004
Accepted: 15 November 2004

References

Abal, M., M. Piel, V. Bouckson-Castaing, M.M. Mogensen, J.-B. Sibarita, and M. Bornens. 2002. Microtubule release from the centrosome in migrating cells. *J. Cell Biol.* 159:731–737.

Ahmad, F.J., and P.W. Baas. 1995. Microtubules released from the neuronal centrosome are transported into the axon. *J. Cell Sci.* 108:2761–2769.

Ahmad, F.J., C.J. Echeverri, R.B. Vallee, and P.W. Baas. 1998. Cytoplasmic dynein and dynactin are required for the transport of microtubules into the axon. *J. Cell Biol.* 140:391–402.

Bacallao, R., C. Antony, C. Dotti, E. Karsenti, E.H.K. Stelzer, and K. Simons. 1989. The subcellular organization of Madin-Darby canine kidney cells during the formation of a polarized epithelium. *J. Cell Biol.* 109:2817–2832.

Bloom, K. 2001. Nuclear migration: cortical anchors for cytoplasmic dynein. *Curr. Biol.* 11:R326–R329.

Canman, J.C., L.A. Cameron, P.S. Maddox, A. Straight, J.S. Tirnauer, T.J. Mitchison, G. Fang, T.M. Kapoor, and E.D. Salmon. 2003. Determining the position of the cell division plane. *Nature.* 424:1074–1078.

Cao, K., R. Nakajima, H.H. Meyer, and Y. Zheng. 2003. The AAA-ATPase Cdc48/p97 regulates spindle disassembly at the end of mitosis. *Cell.* 115:355–367.

Cheeseman, I.M., and A. Desai. 2004. Cell division: AAAtacking the mitotic spindle. *Curr. Biol.* 14:R70–R72.

Compton, D.A. 2000. Spindle assembly in animal cells. *Annu. Rev. Biochem.* 69:95–114.

Glotzer, M. 2004. Cleavage furrow positioning. *J. Cell Biol.* 164:347–351.

Gonczy, P. 2002. Mechanisms of spindle positioning: focus on flies and worms. *Trends Cell Biol.* 12:332–339.

Goodson, H., and P. Wadsworth. 2004. Methods for expressing and analyzing GFP-tubulin and GFP-microtubule-associated proteins. *In* Live Cell Imaging: A Laboratory Manual. R.D. Goldman and D.L. Spector, editors. Cold Spring Harbor Laboratory Press, Cold Spring Harbor, NY. 537–553.

Grill, S.W., J. Howard, E. Schaffer, E.H.K. Stelzer, and A. Hyman. 2003. The distribution of active force generators controls mitotic spindle position. *Science.* 301:518–521.

Karsenti, E., and I. Vernos. 2001. The mitotic spindle: a self-made machine. *Science.* 294:543–547.

Keating, T.J., J.G. Peloquin, V.I. Rodionov, D. Momcilovic, and G.G. Borisy. 1997. Microtubule release from the centrosome. *Proc. Natl. Acad. Sci. USA.* 94:5078–5083.

Khodjakov, A., and C.L. Rieder. 1999. The sudden recruitment of γ-tubulin to the centrosome at the onset of mitosis and its dynamic exchange throughout the cell cycle, do not require microtubules. *J. Cell Biol.* 146:585–596.

Merdes, A., K. Ramyar, J.D. Vechio, and D.W. Cleveland. 1996. A complex of NuMA and cytoplasmic dynein is essential for mitotic spindle assembly. *Cell.* 87:447–458.

Mogensen, M.M., A. Malik, M. Piel, V. Bouckson-Castaing, and M. Bornens. 2000. Microtubule minus-end anchorage at centrosomal and non-centrosomal sites: the role of ninein. *J. Cell Sci.* 113:3013–3023.

Murray, A.W., A.B. Desai, and E.D. Salmon. 1996. Real time observation of anaphase in vitro. *Proc. Natl. Acad. Sci. USA.* 93:12327–12332.

O'Toole, E., K.L. McDonald, J. Mantler, J.R. McIntosh, A. Hyman, and T. Muller-Reichert. 2003. Morphologically distinct microtubule ends in the mitotic centrosome of *Caenorhabditis elegans*. *J. Cell Biol.* 163:451–456.

Patterson, G.H., and J. Lippincott-Schwartz. 2002. A photoactivatable GFP for selective photolabeling of proteins and cells. *Science.* 297:1873–1877.

Piehl, M., and L. Cassimeris. 2003. Organization and dynamics of growing microtubule plus ends during early mitosis. *Mol. Biol. Cell.* 14:916–925.

Piehl, M. U.S. Tulu, P. Wadsworth, and L. Cassimeris. 2004. Centrosome maturation: measurement of microtubule nucleation throughout the cell cycle using GFP-tagged EB1. *Proc. Natl. Acad. Sci. USA.* 101:1584–1588.

Rieder, C.L., and A. Khodjakov. 2003. Mitosis through the microscope: advances in seeing inside live dividing cells. *Science.* 300:91–96.

Rodionov, V.I., and G.G. Borisy. 1997. Microtubule treadmilling in vivo. *Science.* 275:215–218.

Rusan, N.M., C.J. Fagerstrom, A.M. Yvon, and P. Wadsworth. 2001. Cell cycle-dependent changes in microtubule dynamics in living cells expressing green fluorescent protein-α tubulin. *Mol. Biol. Cell.* 12:971–980.

Rusan, N.M., U.S. Tulu, C. Fagerstrom, and P. Wadsworth. 2002. Reorganization of the microtubule array in prophase/prometaphase requires cytoplasmic dynein-dependent microtubule transport. *J. Cell Biol.* 158:997–1003.

Saxton, W.M., D.L. Stemple, R.J. Leslie, E.D. Salmon, M. Zavortink, and J.R. McIntosh. 1984. Tubulin dynamics in cultured mammalian cells. *J. Cell Biol.* 99:2175–2186.

Tulu, U.S., N.M. Rusan, and P. Wadsworth. 2003. Peripheral, non-centrosome-associated microtubules contribute to spindle formation in centrosome-containing cells. *Curr. Biol.* 13:1894–1899.

Verde, F., J.-C. Labbe, M. Doree, and E. Karsenti. 1990. Regulation of microtubule dynamics by cdc2 protein kinase in cell-free extracts of *Xenopus* eggs. *Nature.* 343:233–237.

Wheatley, S.P., E.H. Hinchcliffe, M. Glotzer, A.A. Hyman, G. Sluder, and Y. Wang. 1997. CDK1 inactivation regulates anaphase spindle dynamics and cytokinesis in vivo. *J. Cell Biol.* 138:385–393.

Zhai, Y., P.J. Kronebusch, P.M. Simon, and G.G. Borisy. 1996. Microtubule dynamics at the G2/M transition: abrupt breakdown of cytoplasmic microtubules at nuclear envelope breakdown and implications for spindle morphogenesis. *J. Cell Biol.* 135:201–214.

Zimmerman, S., P.T. Tran, R.R. Daga, O. Niwa, and F. Chang. 2004. Rsp1p, a J domain protein required for disassembly and assembly of microtubule organizing centers during the fission yeast cell cycle. *Dev. Cell.* 6:497–509.